AAPS PharmSciTech (2024) 25:176
https://doi.org/10.1208/s12249-024-02892-w

RESEARCH ARTICLE

Evaluation of Gemcitabine and Epigallocatechin-3-Gallate Loaded Solid Lipid Nanoparticles on Benzopyrene Induced Lung Cancer Model Via Intranasal Route: Improved Pharmacokinetics and Safety Profile

Mohini Mishra[1] · Rinki Verma[2] · Aditya Sharma[3] · Krishan Kumar[1] · Ruchi Chawla[1]

Received: 8 May 2024 / Accepted: 15 July 2024 / Published online: 31 July 2024

Abstract

The objective of this study was to create a new treatment for lung cancer using solid lipid nanoparticles (SLNs) loaded with gemcitabine (GEM) and epigallocatechin-3-gallate (EGCG) that can be administered through the nose. We analyzed the formulation for its effectiveness in terms of micromeritics, drug release, and anti-cancer activity in the benzopyrene-induced Swiss albino mice lung cancer model. We also assessed the pharmacokinetics, biodistribution, biocompatibility, and hemocompatibility of GEM-EGCG SLNs. The GEM-EGCG SLNs had an average particle size of 93.54 ± 11.02 nm, a polydispersity index of 0.146 ± 0.05, and a zeta potential of -34.7 ± 0.4 mV. The entrapment efficiency of GEM and EGCG was 93.39 ± 4.2% and 89.49 ± 5.1%, respectively, with a sustained release profile for both drugs. GEM-EGCG SLNs had better pharmacokinetics than other treatments, and a high drug targeting index value of 17.605 for GEM and 2.118 for EGCG, indicating their effectiveness in targeting the lungs. Blank SLNs showed no pathological lesions in the liver, kidney, and nasal region validating the safety of SLNs. GEM-EGCG SLNs also showed fewer pathological lesions than other treatments and a lower hemolysis rate of 1.62 ± 0.10%. These results suggest that GEM-EGCG SLNs could effectively treat lung cancer.

Keywords biodistribution · epigallocatechin-3-gallate · gemcitabine · intranasal · IVIS · lung cancer · pharmacokinetic · solid lipid nanoparticles

Introduction

Lung cancer represents one of the most common causes of death related to cancer around the world [1]. According to Cancer Statistics, 2024, published in CA: A Cancer Journal for Clinicians, 2,001,140 new cases of cancer have been reported with 611,720 deaths due to cancer in the United States and nearly 1680 deaths per day [2]. The greatest number of deaths are reported to be due to lung cancer [3] which is reported to be more than breast cancer, prostate cancer, pancreatic cancer, and colorectal cancer [4]. As per reports of Cancer Statistics 2024, the reason for 101,300 of the 125,070 lung cancer deaths in 2024 will be cigarette smoking with an additional 3500 lung cancer deaths caused by passive smoking [2]. The main etiology reported for the manifestation of lung cancer is tobacco smoking in the United States or other countries where smoking is a common practice. Years of subjection to tobacco smoke leads to structural damage in the lungs which emerges as chronic obstructive pulmonary disease and emphysema [5]. Bronchial epithelium represents a concatenation of morphological alterations starting from basal cell hyperplasia to metaplasia followed by severe dysplasia to carcinoma *in situ* leading to frank carcinoma at a late stage [6]. The concatenation of changes is characteristic of the squamous subtype of non-small cell lung cancer whereas adenocarcinomas are primarily the dominant subtype in cases of low carcinogen subjection or non-smokers with some cases of exceptions of adenocarcinomas in subjects with heavy carcinogen exposure too [7]. Atypical adenomatous hyperplasia is less well

✉ Ruchi Chawla
rchawla.phe@iitbhu.ac.in

[1] Department of Pharmaceutical Engineering & Technology, Indian Institute of Technology (BHU), Varanasi, Uttar Pradesh 221005, India

[2] Department of Biomedical Engineering, Indian Institute of Technology (BHU), Varanasi, Uttar Pradesh 221005, India

[3] Sri Ganganagar Homoeopathic Medical College, Hospital & Research Center, Tantia University, Sri Ganganagar, Rajasthan 335002, India

characterized with premalignant lesions associated with adenocarcinomas [8].

Gemcitabine (GEM) belongs to the class of pyrimidine analogues, chemically it is 2',2'-difluorodeoxycytidine, which is a cytidine analogue with hydroxyl groups on ribose sugar replaced by two fluorine atoms [9]. GEM is one of the globally prescribed anticancer drugs widely used in the treatment of pancreatic cancer along with ovarian cancer, breast cancer, non-small cell lung cancer, and bladder cancer, in combination with other anticancer agents like cisplatin [10]. The hydrophilicity of GEM limits its diffusion across biological membranes and is transported via nucleoside transporters present in the membrane to the cells [11]. It has been reported that 10% of the unchanged GEM undergoes renal filtration by the kidney, and more than 90% of the administered dose is usually recovered within 1 week of administration in urine in the form of 2',2'-difluoro-deoxyuridine (99%) or GEM (1%) [12]. GEM is also degraded by the plasma deaminase and because of its rapid degradation and elimination from the body, a large dose of GEM is required to meet the therapeutic efficiency which results in toxic side effects [13].

Natural compounds have gained attention in preventing and treating various diseases due to the side effects and resistance associated with synthetic compounds [14]. These natural compounds have validated their importance by being used along with conventional formulations for the effective treatment of cancer, neurological disorders, and cardiovascular diseases [15]. Medicinal plants have obvious merits over later in terms of diminished toxicity and of course accentuation [16]. Hence, natural compounds can be added along with conventional synthetic compounds to potentiate the therapeutic efficacy of the chemotherapeutic compounds. Epigallocatechin-3-gallate (EGCG) is a polyphenolic compound present in the tea (*Camellia sinensis*) leaves [17]. Apart from EGCG, epigallocatechin, epicatechin gallate, and epicatechin are other polyphenols present in green tea which in total constitute 30 to 42% of water-soluble solids in green tea [18]. EGCG is reported to have therapeutic efficacy against cardiovascular diseases and cancer [18]. The liver and small intestine are the major organs involved in the absorption followed by the metabolism of EGCG and the metabolic fate of EGCG involves glucuronidation, methylation, and sulfation reactions [19]. Chen et al., have reported the efficacy of EGCG against lung cancer, loaded in gelatin nanoparticles along with cisplatin anti-cancer drug, and evaluated the synergistic effect exhibited by these two drugs against lung cancer (14). Another research group, Tang et al., have prepared honokiol nanoparticles of EGCG functionalized chitin and reported enhanced tumour selectivity with a significant reduction in tumour growth and no toxic effects *in vitro* and *in vivo* liver cancer models [20].

Interest in lipid-based drug delivery systems is not new and their origin can be traced back to 1965 when liposomes were discovered by biochemist 'Bangham' [21]. Solid lipid nanoparticles are a colloidal carrier system encompassing solid lipid, water, and surfactant. Solid fat or lipids include fatty acids, waxes, steroids, monoglycerides, diglycerides as well and triglycerides and the limit for their concentration ranges between 0.1–30% w/w of the formulation [21]. The obvious merits of SLNs over nanoemulsions and polymer-based nanoparticles are enhanced stability of the drug, accentuated drug entrapment efficiency, and biocompatibility as these are mostly formulated from biodegradable and generally regarded as safe (GRAS) certified excipients. Apart from these merits SLNs also command the advantages of encapsulated drug release and avert premature degradation of the drug in the system [22, 23].

Researchers exploring the therapeutic potentials of EGCG have reported that EGCG not only acts as a chemopreventive agent but also as a chemotherapeutic agent against a wide array of cancer cell lines. Inhibition of tumorigenesis, proliferation, and angiogenesis has been attributed as the anticancer mechanism exhibited by EGCG. EGCG exhibits its anticancer effects by multiple pathways in different type of cancers [22]. However, the compromised bioavailability and stability of EGCG obstructed its clinical application as a therapeutic agent. Novel drug delivery systems-based formulation approaches could amplify its solubility and pharmacokinetic profile. On the other hand, conventional treatment approaches for lung cancer offer not so satisfactory results and a compromised life associated with potential side effects of chemotherapy, radiation therapy, and surgical resection. In the absence of targeted therapies, systemic administration of chemotherapy exposes normal cells to these potent chemotherapeutic drugs resulting in the inhibition of their growth making the patient weak and eventually leading to death. Therefore, a drug regimen of combining the chemotherapeutic drugs with a phytoconstituent would subsequently lead to cutting short the dose of chemotherapeutic agents and will act synergistically to alleviate the condition of lung cancer and diminished dose-dependent side effects of chemotherapeutic agents [16, 24–26].

In the present study, an anti-cancer-targeted drug delivery system via intranasal route has been developed. Intranasal administration is a non-invasive as well as patient-compliant technique that will help in the targeted delivery of drugs to the lungs, thereby reducing the dose and dose-dependent side effects and metabolic degradation as compared to the intravenous route of administration [27]. It may also help reduce the dose-dependent side effects of GEM which undergo rapid degradation via the liver and kidney. Our approach is to develop an intranasal GEM and EGCG-loaded lipid-based formulation and evaluate its anti-cancer efficacy, targeting potential, and biocompatibility in lung cancer. The

putative mechanism of GEM-EGCG SLNs as anticancer agent has been diagrammatically represented in Fig. 1. Upon reaching the tumor site GEM-EGCG SLNs are selectively internalized by the endocytosis [28] and enhanced permeability & retention effect (EPR) [29] into the tumor cells. GEM-EGCG SLNs exhibit their anti-cancer effect by induction of apoptosis [30–32], inhibition of tumorigenesis and proliferation along with inhibition of angiogenesis in tumor cells [33–35]. GEM-EGCG SLNs also inhibit DNA synthesis and its repair [9].

Materials & Methods

Materials

Glycerol monostearate (GMS) was received as a kind gift sample from Fine Organics, Fine House, Mumbai, India. Gemcitabine (GEM) ex gratis sample from Neon labs; polyvinyl alcohol (PVA) and dialysis membrane-70 were procured from HiMedia Laboratories Pvt. Ltd., Mumbai, India. Pluronic F-127 (PF-127), benzopyrene (B(a)P), and epigallocatechin-3-gallate (EGCG) were procured from Sigma Aldrich. Hydrogenated soy phosphatidylcholine (HSPC) was received from Lipoid GmBH, Germany; dichloromethane was purchased from Merck Life Sciences Private Limited, Mumbai, India, and chloroform was procured from Thermo Fisher Scientific India Pvt. Ltd.

Methods

Synthesis of Solid Lipid Nanoparticles

Glycerol monostearate (200 mg) and hydrogenated soy phosphatidylcholine (50 mg) were dissolved in 5 mL of the organic solvent (dichloromethane), forming the lipid phase of the formulation. Equivalent dose of Gemcitabine (3 mg/kg) [36] and epigallocatechin-3-gallate (15 mg/kg) [37] were dissolved in 2 mL of HPLC water and further added into the lipid phase along with 4 mL of 1% w/v polyvinyl alcohol solution under homogenization (IKA® T18 digital ULTRA TURRAX®) at 12,000 rpm for 10 min followed by ultrasonication for 5 min in bath sonicator. The resultant primary emulsion was further added into 4 mL of 1% w/v Pluronic F-127 solution and then homogenized (IKA® T18 digital ULTRA TURRAX®) at 12,000 rpm for 10 min which was further subjected to a second cycle of ultrasonication for 5 min in bath sonicator leading to the formation of double emulsion (W/O/W). The formulation was then kept on a magnetic stirrer at 1000 rpm for 3 h for the complete removal of organic solvent [38]. Similarly, blank SLNs, GEM SLNs, and EGCG SLNs were prepared by employing a double emulsification solvent evaporation technique.

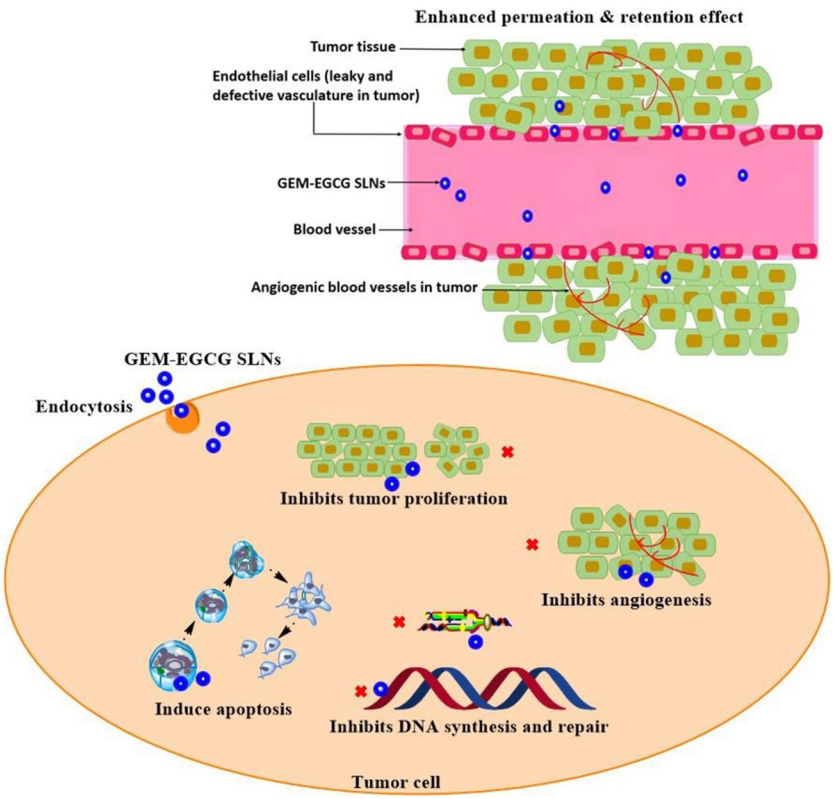

Fig. 1 Putative mechanism of GEM-EGCG SLNs as anticancer agent

Characterization

Micromeritics and zeta potential analysis was carried out on Malvern Zetasizer Pro (Malvern, UK) at Biophysics & Nanotechnology Lab, Department of Physics, IIT BHU, Varanasi, India. Particle size and polydispersity index (PDI) were determined using dynamic light scattering at an angle of 90°, a refractive index of 1.45, and a cell temperature of 25° C. The samples were diluted in a ratio of 1:10 with distilled water and transferred to the cell ZEN1002 for analysis. The zeta potential of the samples was determined by the electrophoretic light scattering phenomenon in zeta potential dip cell MAL1251975. All the studies were carried out in triplicate [27]. Entrapment efficiency was determined by the dialysis membrane method [39–41]. 2 mL of the formulation was transferred into the dialysis bag (12 kDa) suspended in 100 mL of distilled water which was kept on a magnetic stirrer at 400 rpm for two hours [42]. After two hours, a 2 mL aliquot was withdrawn and analyzed by reverse phase UV-HPLC (Agilent Technologies 1260 Infinity II, Quasar C18 250 × 4.6 mm 5 µm column) method. With an injection volume of 20 µL, chromatographic conditions used for analysis were a flow rate of 0.7 mL/min and λ_{max} 268 nm for GEM and 280 nm for EGCG with a retention time of 6 min. The mobile phase used for GEM was acetonitrile: water (50:50) and EGCG was acetonitrile: acetic acid (0.4% v/v). The entrapment efficiency was calculated as per the following formula.

$$Percent\ entrapment\ efficiency = \frac{Amount\ of\ entrapped\ drug}{Theoretical\ amount\ of\ drug\ in\ the\ dialysis\ bag} \times 100 \quad (1)$$

where, the amount of entrapped drug = Theoretical amount of drug in the dialysis bag – the amount of free drug in the dialysis medium.

Drug release studies were performed in phosphate buffer pH 5.5 [43–46] for 48 h. 1 mL of each of GEM-EGCG SLNs, GEM SLNs, and EGCG SLNs, was filled in a dialysis bag (12 kDa) and transferred into 100 mL of release medium of phosphate buffer pH 5.5 under constant stirring at 400 rpm. The sink conditions were maintained by adding 2 mL of phosphate buffer pH 5.5 post-withdrawal of 2 mL aliquots at time points: 0 min, 5 min, 10 min, 15 min, 30 min, 45 min, 1 h, 2 h, 4 h, 6 h, 8 h, 10 h, 12 h, 24 h, 36 h, and 48 h [42]. The aliquots withdrawn were analyzed under the UV-HPLC method for the determination of the amount of drug (GEM and EGCG) present in them and further calculations were done to estimate the pattern of drug release from different formulations.

Animal Studies

The ethical approval was obtained from the IAEC of the Indian Institute of Technology, Banaras Hindu University, Varanasi (IAEC approval number IIT(BHU)/IAEC/2023/058).

Healthy female Swiss Albino mice, 30 ± 10 g, 6–8 weeks, and female Wistar rats, 250 g ± 10 g, 7–9 weeks, were procured from the central animal house of the Institute of Medical Sciences, Banaras Hindu University (IMS BHU). All the animals were housed in the animal house facility present in the Department of Pharmaceutical Engineering & Technology, Indian Institute of Technology, BHU, Varanasi, India, under standard laboratory conditions (temperature: 25 °C ± 2 °C; relative humidity: 40% ± 5%; and 12 h light/dark cycle) provided with proper access to drinking water and animal feed *ad libitum.* The animals were caged in polypropylene cages with proper animal bedding which was regularly replaced to avoid unhygienic conditions and animals were allowed to adapt to the laboratory conditions for a week before the commencement of the experimental study.

Development of Lung Cancer Animal Model

Benzopyrene (B(a)P) is a polycyclic aromatic hydrocarbon that is present in cigarette smoke, foodstuffs, and air polluted by industrial wastes and emissions from automobiles [47]. A level of less than 10 ng is reported to be present in a cigarette [48] and a level of 76 ng in foodstuffs [49]. In the liver and lung, B(a)P is metabolized into benzopyrene-7,8-diol-9,10-epoxide with the help of metabolizing enzymes cytochrome P450 1A1/1A2, and cytochrome P450 1B1 [50]. Benzopyrene-7,8-diol-9,10-epoxide reacts with DNA at the N_2 position of guanine and results in the production of DNA adduct responsible for carcinogenesis [47, 50, 51]. We induced lung cancer in female Swiss albino mice with B[a]P, which is reported to have a 100% induction rate in Swiss albino mice [52]. B[a]P dissolved in olive oil was administered to each mice by oral gavage at a dose of 100 mg/kg, twice a week for one month [52, 53]. All the animals were weighed and documented twice a week regularly till the completion of the study.

Experimental Study Design

A randomized set of 48 female Swiss albino mice was employed for the evaluation of the anti-cancer activity of

GEM-EGCG SLNs. The animals were divided into eight groups, each containing 6 female Swiss albino mice provided with proper access to drinking water and food *ad libitum*. Groups 2 to 8 uniformly received B[a]P for the first month of study.

Group 1 (Normal control): This group received normal drinking water and food *ad libitum*.
Group 2 (B[a]P): This group was treated with B[a]P, twice a week (Monday and Thursday) for one month.
Group 3 (B[a]P + GEM-EGCG SLNs): This group received intranasal instillation (50 µL was instilled with the help of a micropipette into the nostrils slowly drop by drop to partially anesthetized mice) of GEM-EGCG SLNs twice a week for two months.
Group 4 (B[a]P + GEM SLNs): The animals were instilled in GEM SLNs (3 mg/kg) intranasally twice a week for a period of two months.
Group 5 (B[a]P + EGCG SLNs): From the second month the animals received EGCG SLNs (15 mg/kg) intranasally twice a week for a period of two months.
Group 6 (B[a]P + Blank SLNs): The animals received blank SLNs intranasally twice a week for a period of two months.
Group 7 (B[a]P + GEM): GEM (3 mg/kg) was administered intranasally twice a week for a period of two months.
Group 8 (B[a]P + EGCG): The animals received B[a]P in the first month and from the second-month intranasal instillation of EGCG (15 mg/kg) twice a week for a period of two months.

All the experimental animals were weighed twice a week and the weight was documented till the completion of the study.

Pharmacokinetic Study

Female Wistar rats, 250 g ± 10 g, were randomly divided into five groups ($n = 6$) for the pharmacokinetic study of GEM-EGCG SLNs, GEM SLNs, EGCG SLNs, pure GEM solubilized in PBS 7.4, and pure EGCG solubilized in PBS 7.4.

Plasma Pharmacokinetic For plasma pharmacokinetic studies, the first group was administered with GEM-EGCG SLNs; the second group was given GEM SLNs; the third group was administered with EGCG SLNs; the fourth group was administered with GEM solubilized in PBS 7.4; and the fifth group received EGCG solubilized in PBS 7.4 (50 µL volume [54] of the respective formulations comprising GEM and EGCG at a dose of 3 mg/Kg and 15 mg/Kg, respectively were given through intranasal instillation to rats [37, 55, 56]). Blood aliquots (0.5 mL) were amassed from the tail vein at specified time intervals: 0 min, 5 min, 15 min, 30 min, 1 h, 2 h, 4 h, 8 h, 12 h, and 24 h. The aliquots withdrawn were treated by adding acetonitrile to precipitate out the plasma proteins followed by centrifugation at 12,000 rpm for 10 min. The clear supernatant was collected and filtered and the concentration of GEM and EGCG was estimated by reverse phase UV-HPLC (Agilent Technologies 1260 Infinity II, Quasar C18 250 × 4.6 mm 5 µm column) method. With an injection volume of 20 µL, chromatographic conditions used for analysis were a flow rate of 0.7 mL/min and λ_{max} 268 nm for GEM and 280 nm for EGCG with a retention time of 6 min. The mobile phase used for GEM was acetonitrile: water (50:50) and EGCG was acetonitrile: acetic acid (0.4% v/v).

Lung Pharmacokinetics For lung pharmacokinetic profiling, formulations were administered intranasally to the female Wistar rats similarly as described above in Sect. 2.2.6.1. The animals were sacrificed at 5 min, 15 min, 30 min, 1 h, 4 h, and 8 h from each group, and lungs were excised and stored in liquid nitrogen at – 80° C. Lung sample weighing equal to 1.0 g was cut into small pieces and incubated with 2.0 mL of PBS solution. Then, the incubated sample was homogenized for 2 min at 4℃ followed by centrifugation of the homogenate at 12,000 rpm for 10 min. The supernatant was taken out and mixed with acetonitrile to precipitate out the proteins. The mixture was centrifuged at 12,000 rpm for 10 min. The clear supernatant was collected and the content of GEM and EGCG were analyzed by the UV-HPLC method as described in Plasma Pharmacokinetic Study [54].

Lung targeting efficiency of the intranasal route

Drug Targeting Index The pharmacokinetic parameter which quantifies the target efficiency of the route of administration to deliver the drug of choice at the target site as compared to the systemic route gives the drug targeting index (DTI) [57]. In the present research, DTI is the ratio of area under the curve (AUC) in lungs and plasma following intranasal (i.n.) administration divided by the AUC in lungs and plasma after intravenous (i.v.) administration [58].

$$Drug\ targeting\ index\ (DTI) = \frac{\frac{(AUC\ lungs)i.n.}{(AUC\ plasma)i.n.}}{\frac{(AUC\ lungs)i.v}{(AUC\ plasma)i.v.}} \quad (2)$$

Plasma and lung pharmacokinetics were studied upon intravenous administration of GEM-EGCG SLNs. We administered an intravenous bolus of GEM-EGCG SLNs through the lateral tail vein into the female Wistar rats at an equivalent dose to that of intranasal administration. For the calculation of pharmacokinetic parameters in plasma, blood aliquots

(0.5 mL) were amassed from the tail vein at specified time intervals: 0 min, 5 min, 15 min, 30 min, 1 h, 2 h, 4 h, and 8 h. The aliquots withdrawn were treated and the concentration of GEM and EGCG was estimated by reverse phase UV-HPLC method.

For calculation of pharmacokinetic parameters in the lungs, we administered i.v. bolus GEM-EGCG SLNs through the lateral tail vein into the female Wistar rats at an equivalent dose as that of intranasal administration, and then animals were sacrificed at 5 min, 15 min, 30 min, 1 h, 4 h, and 8 h from each group and lungs were excised and stored in liquid nitrogen at – 80° C till GEM and EGCG content was analyzed by UV-HPLC method.

IVIS- *In Vivo* Imaging System The *in vivo* imaging in Swiss albino mice after intranasal instillation of GEM-EGCG SLNs was performed by Photon Imager Optima V4 – Biospace Lab (Photon Acquisition 3.6 software) and images were analyzed by M_3 Vision analysis software. Partially anesthetized animals were given with intranasal instillation of GEM-EGCG SLNs. The animals were anesthetized and placed on the sample stage in the IVIS imaging system at time points 0, 1, 2, 6, 24, and 48 h and images were collected [59].

Biodistribution Study

A biodistribution study is a direct indication of the targeting efficiency of a pharmaceutical formulation, which also indicates the selective accumulation of prepared formulations in different body organs and their metabolic sites as well. We employed female Wistar rats 250 g ± 10 g to carry out the biodistribution study. The animals were randomly divided into five groups and intranasally administrated with GEM-EGCG SLNs, GEM SLNs, EGCG SLNs, GEM solubilized in PBS 7.4, and EGCG solubilized in PBS 7.4. Rats from each group were sacrificed at 1 h and 6 h intervals and the liver, lungs, kidney, heart, and spleen were excised out from the body, wiped, and stored in 10% formalin solution. A weighed portion of the tissue sample was homogenized and vortexed for 1 min followed by the addition of acetonitrile to the sample. All samples were centrifuged at 12,000 rpm for 10 min, clear supernatant was collected and evaluated by UV-HPLC to estimate the amount of GEM and EGCG in different organs [46].

Histopathological Study

A histopathological study was performed on the treatment groups. After the termination of the study, animals were sacrificed, and post-mortem analysis was done. Lungs were excised carefully, washed, and stored under 10% formalin solution for 24 h. Once the tissues were fixed, a portion from the lungs was positioned in a tissue cassette followed by setting or embedment in a paraffin block. Microscope slides were prepared by cutting 5 µm thick sections of tissues and then stained with eosin and hematoxylin stain. The slides were studied and analyzed under an optical microscope (Magnus MLX Plus).

Assessment of Safety and Biocompatibility of SLNs

Assessment of the safety of the SLNs was performed in Swiss albino mice. Two groups each with 6 female Swiss albino mice were respectively given saline control and blank SLNs via intranasal route of administration for two months twice a week. After the termination of the study, histopathological sections of the liver and kidney [60] were prepared in the same manner as described in Sect. 2.2.9. The slides were observed under the optical microscope (Magnus MLX Plus).

Next, we conducted a safety assessment of GEM-EGCG SLNs in the nasal region of Swiss albino mice. Histopathological sections of the nasal mucosa of the treatment group receiving GEM-EGCG SLNs and a normal control group were prepared as described in Sect. 2.2.9 and the slides were observed under the optical microscope (Magnus MLX Plus).

Hemolysis can be understood as the rupturing of red blood cells followed by the release of hemoglobin into blood plasma. Hemolysis can further result in jaundice and anemia, hence, assessment of the biocompatibility of nanoparticles is suggested as nanoparticles can likely interact with blood cells owing to their small size as compared to conventional dosage forms [61]. Assessment of biocompatibility of GEM-EGCG SLNs, GEM, and EGCG with blood was studied by hemolysis study. Fresh blood was collected from Swiss albino mice through the tail vein. The blood cells were separated by centrifuging the whole blood at 12,000 rpm at 4 ℃ for 10 min. The supernatant was pipetted out and the blood erythrocyte cells were washed with normal saline followed by two more cycles of centrifugation at 12,000 rpm at 4 ℃ for 10 min with normal saline. Again, the supernatant was pipetted out and blood erythrocyte cells were collected and diluted with 1 mL of normal saline. Dilutions equivalent to 25, 50, 75, 100, and 125 µg/mL of GEM-EGCG SLNs, GEM, and EGCG were prepared in normal saline.1% v/v of Triton X-100 in normal saline was fixed as positive control (PC) and normal saline as negative control (NC). 100 µL of blood erythrocyte cells were mixed with 900 µL of varying dilutions of GEM-EGCG SLNs, GEM, and EGCG and incubated for one hour followed by centrifugation at 10,000 rpm for 10 min. The supernatant was analyzed under a microplate reader (Spectra Max M5, Molecular Devices (SoftMax Pro 7.1.2 Data Acquisition and Analysis Software) at 540 nm [62].

$$Hemolysis\ rate\ (\%) = \frac{Dt - Dnc}{Dpc - Dnc} \times 100 \quad (3)$$

where Dt is the absorbance of the test sample; Dnc is the absorbance of the negative control; and Dpc is the absorbance of the positive control.

Statistical Analysis

The statistical analysis was done using Graph Pad Prism software (trial version 9.5.1, Graph Pad software, CA, USA). The results obtained were represented as mean ± standard deviation for the demonstrated number of experimental runs. The data was analyzed by ANOVA (one-way and two-way) and non-parametric comparisons. Values of $p < 0.001$, $p < 0.01$, and $p < 0.05$ were deemed as statistically extremely significant, highly significant, and significant, respectively. The value of $p > 0.05$ was deemed as statistically non-significant.

Results & Discussion

Characterization

Particle size has a direct effect on lung deposition, the smaller the particle size (less than 10 µm [63]) better the penetration and deposition in the lungs [64, 65] whereas larger-sized particles are obstructed in the upper airways and are employed for the treatment of medical conditions of the upper respiratory region. It has been reported that particles having sizes in the range of 5 µm to 10 µm target the oropharyngeal region and large conducting airways [66] whereas particles with sizes of 1 µm to 5 µm are deposited in the alveolar region and small airways [67]. Particles with a particle size of less than 3 µm have more than an 80% of chance reaching lower respiratory regions with more than 60% of deposition in the alveoli [64, 68]. Particles having a size less than 1 µm are reported to have higher pulmonary distribution and reach into distal airways [65]. For any colloidal system, zeta potential values govern their electrostatic stability, zeta potential values greater than ± 30 mV result in electrostatic stable systems. Several studies have reported that zeta potential has a significant impact on drug retention in the nasal mucosa region. Mucin found in the nasal mucosa bears a negative charge, hence formulations with positive zeta potential value result in better electrostatic attraction and facilitate longer retention time, and enhance the attachment with nasal mucosa [69–72]. GEM-EGCG SLNs have shown a zeta potential value of -34.7 ± 0.4 mV, a negative value of zeta potential demonstrates repulsion between the negatively charged mucin in the nasal mucosa and GEM-EGCG SLNs and hence GEM-EGCG SLNs could have traversed into the respiratory region with ease in the absence of any electrostatic attraction or attachment. The high value of zeta potential also reflects the stability of the GEM-EGCG SLNs. Micromeritic studies revealed a mean particle size in the range of 93.54 ± 11.02 nm with a polydispersity index (PDI) of 0.146 ± 0.05 and a zeta potential value of -34.7 ± 0.4 mV. The particle size was found to be in the nano range and the value of PDI suggested the formation of monodisperse particles [73]. Percent entrapment efficiency as determined by the equilibrium dialysis method was found to be 93.39 ± 4.2% for GEM and 89.49 ± 5.1% for EGCG. The high percent entrapment efficiency could be attributed to the incorporation of GEM and EGCG in the inner hydrophilic core of the nanoparticles. Drug release studies showed sustained drug release of GEM and EGCG for the study period. From Fig. 2(b), it can be inferred that GEM SLNs exhibited higher drug release of GEM as compared to GEM-EGCG SLNs which could be due to the presence of only one drug GEM in GEM SLNs as against the presence of two drugs in GEM-EGCG SLNs which might interfere with the release characteristics of each other in the release media. Similarly, higher release was noticed from EGCG SLNs in comparison to GEM-EGCG SLNs.

Pharmacokinetic Study

Pharmacokinetics (Lung & Plasma)

Female Wistar rats, 250 g ± 10 g, were employed to study the pharmacokinetic profiles of GEM-EGCG SLNs, GEM SLNs, EGCG SLNs, pure GEM solubilized in PBS 7.4, and pure EGCG solubilized in PBS 7.4 in plasma and lungs. The various pharmacokinetic parameters for GEM and EGCG in plasma and lungs were evaluated by Kinetica 5.0 PK/PD Analysis software (Thermo Fisher Scientific). The various pharmacokinetic parameters have been mentioned in Tables I and II. It was found that GEM-EGCG SLNs showed an 18.2-fold increase in $t_{1/2}$ as compared to pure GEM and a 9.2-fold increase concerning GEM SLNs for the drug GEM. Whereas for the drug EGCG, GEM-EGCG SLNs showed an increase of 1.62-fold and 8.9-fold in the $t_{1/2}$ concerning EGCG SLNs and pure EGCG, respectively. The increase in the $t_{1/2}$ (which is defined as the time required for half of the drug to be excreted out from the body) could be accounted for to sustained release of GEM and EGCG into the plasma from the SLNs.

Similarly, mean residence time (MRT) showed a pattern similar to that of $t_{1/2}$ for different formulations. It is comprehensible from Table I that for the drug GEM, an approximately 17 times increase in MRT was noticed for GEM-EGCG SLNs as compared to GEM SLNs, and 19.85-fold higher MRT for GEM-EGCG SLNs for pure GEM was observed. For EGCG a 1.64-fold escalation in

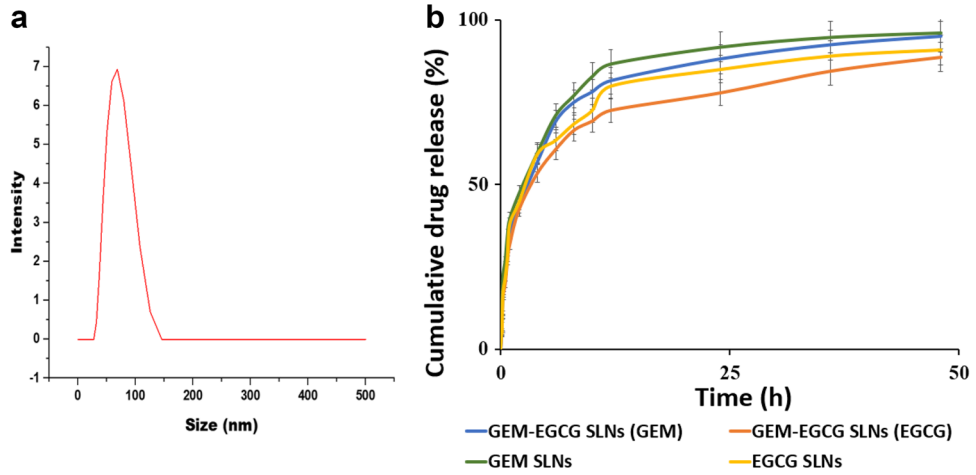

Fig. 2 This figure illustrates **a** the average particle size distribution of particles in GEM-EGCG SLNs, and **b** a graph representing cumulative drug release profile at different time points for GEM-EGCG SLNs (GEM), GEM-EGCG SLNs (EGCG), GEM SLNs, and EGCG SLNs (abbreviations: GEM-EGCG SLNs- gemcitabine and epigallocatechin-3-gallate loaded solid lipid nanoparticles; GEM SLNs- gemcitabine loaded solid lipid nanoparticles; EGCG SLNs- epigallocatechin-3-gallate loaded solid lipid nanoparticles)

Table I Table enlisting pharmacokinetic parameters for GEM and EGCG in plasma upon intranasal administration

S.No	Drug	Formulation	T_{max} (h)	$t_{½}$ (h)	MRT (h)	Clearance (mL/h)	V_D (L)	AUC (µg/µL*h)
1	GEM (Plasma)	GEM-EGCG SLNs	1	272.4	386.92	0.298	0.12	2.514
		GEM SLNs	1	29.7	22.85	3.101	0.27	0.249
		Pure GEM	0.5	14.9	19.49	7.642	0.33	0.098
2	EGCG (Plasma)	GEM-EGCG SLNs	0.5	94.9	134.06	1.872	0.198	2.003
		EGCG SLNs	0.5	58.7	81.68	2.339	0.247	1.603
		Pure EGCG	0.5	10.7	10.34	16.020	0.256	0.234

GEM gemcitabine, *EGCG* epigallocatechin-3-gallate, *GEM-EGCG SLNs* gemcitabine and epigallocatechin-3-gallate loaded solid lipid nanoparticles, *GEM SLNs* gemcitabine loaded solid lipid nanoparticles. *EGCG SLNs* epigallocatechin-3-gallate loaded solid lipid nanoparticles

Table II Table enlisting pharmacokinetic parameters for GEM and EGCG in lungs upon intranasal administration

S.No	Drug	Formulation	T_{max} (h)	$t_{½}$ (h)	MRT (h)	Clearance (mL/h)	AUC (µg/µL*h)
1	GEM (Lungs)	GEM-EGCG SLNs	0.5	87.7	126.40	0.261	2.871
		GEM SLNs	0.5	18.4	27.03	0.926	0.810
		Pure GEM	0.083	1.2	1.48	1.174	0.064
2	EGCG (Lungs)	GEM-EGCG SLNs	0.5	8.0	11.76	7.421	0.505
		EGCG SLNs	0.5	7.7	11.31	6.638	0.565
		Pure EGCG	0.083	2.0	2.81	18.781	0.201

GEM gemcitabine, *EGCG* epigallocatechin-3-gallate, *GEM-EGCG SLNs* gemcitabine and epigallocatechin-3-gallate loaded solid lipid nanoparticles, *GEM SLNs* gemcitabine loaded solid lipid nanoparticles, *EGCG SLNs* epigallocatechin-3-gallate loaded solid lipid nanoparticles

MRT was observed for GEM-EGCG SLNs in comparison to EGCG SLNs and 12.9-fold for GEM-EGCG SLNs and pure EGCG. An escalation in the values of MRT for GEM-EGCG SLNs could be attributed to the long circulation of these nanoparticles in the systemic circulation due to the enhanced permeability and retention (EPR) effect and sustained and regulated release of these drugs from the SLNs into the bloodstream [29]. A better pharmacokinetic profile can improve the therapeutic activity of the drugs. The slower the rate of clearance of a drug from the body, the better the chances for a good therapeutic effect because the drug will be available for a longer duration of time in the body. In other words, MRT and rate of clearance have an inverse relation between them. GEM-EGCG SLNs showed

a tenfold decrease in the rate of clearance in comparison to GEM SLNs whereas, from Table I, it is evident that for the drug EGCG, a fall off of 1.25 and 8.56-fold respectively was observed for GEM-EGCCG SLNs in comparison to EGCG SLNs and pure EGCG. A 2.25 and 2.75-fold decline in the volume of distribution (V_D) was observed for GEM-EGCG SLNs in comparison to GEM SLNs and pure GEM, respectively for the drug GEM, whereas, for the drug EGCG, GEM-EGCG SLNs showed 1.21 and 1.29-fold decrease for EGCG SLNs and pure EGCG. The fall in the value of V_D for GEM-EGCG SLNs indicates lower biodistribution and in turn would probably lead to lower associated toxicity of GEM and EGCG in various body organs which in turn also indirectly corroborates the targeting efficiency of intranasal administration of GEM-EGCG SLNs into lungs. The value of area under the curve (AUC) was found to be the highest for GEM-EGCG SLNs in the case of both the drugs i.e., GEM and EGCG concerning GEM SLNs, EGCG SLNs, pure GEM, and pure EGCG. Higher AUC supports the slower clearance of drugs from the body and greater residence of the drugs in the body.

Table I, enlists different Pharmacokinetic parameters for GEM and EGCG in the lungs upon intranasal administration, it is comprehensible that C_{max} in the lungs was attained faster as compared to that of plasma suggesting faster onset of action of GEM and EGCG in the lungs. From Fig. 3(c), it can be seen that an escalation in the value of $AUC_{0\text{-}8}$ (AUC for the time points 0–8 h) was noticed for GEM and EGCG in the lungs as compared to that of plasma for the drug-loaded SLNs formulations (GEM-EGCG SLNs, GEM SLNs, and EGCG SLNs). This could be due to a slower rate of clearance from the lungs or re-entry of GEM and EGCG into the lungs via the pulmonary artery from the heart [74].

Lung Targeting Efficiency of Intranasal Route

Drug Targeting Index

DTI was quantified for GEM-EGCG SLNs in lungs and plasma upon intranasal and intravenous administration (Fig. 3(b)). The calculated values for DTI show a predominance of intranasal administration over intravenous route of administration with a DTI value of 17.605 for GEM and 2.118 for EGCG. It has been reported that DTI greater than 1 corresponds to the predominant reach of a drug to the target site [57]. It can be inferred from the DTI that intranasal administration of GEM-EGCG SLNs could be adopted as a targeted therapeutic approach against lung cancer which is of course non-invasive as well as patient-compliant. The greater value of DTI in the case of GEM could be attributed to the fact that a greater proportion of GEM after intravenous administration is rapidly distributed to different body organs

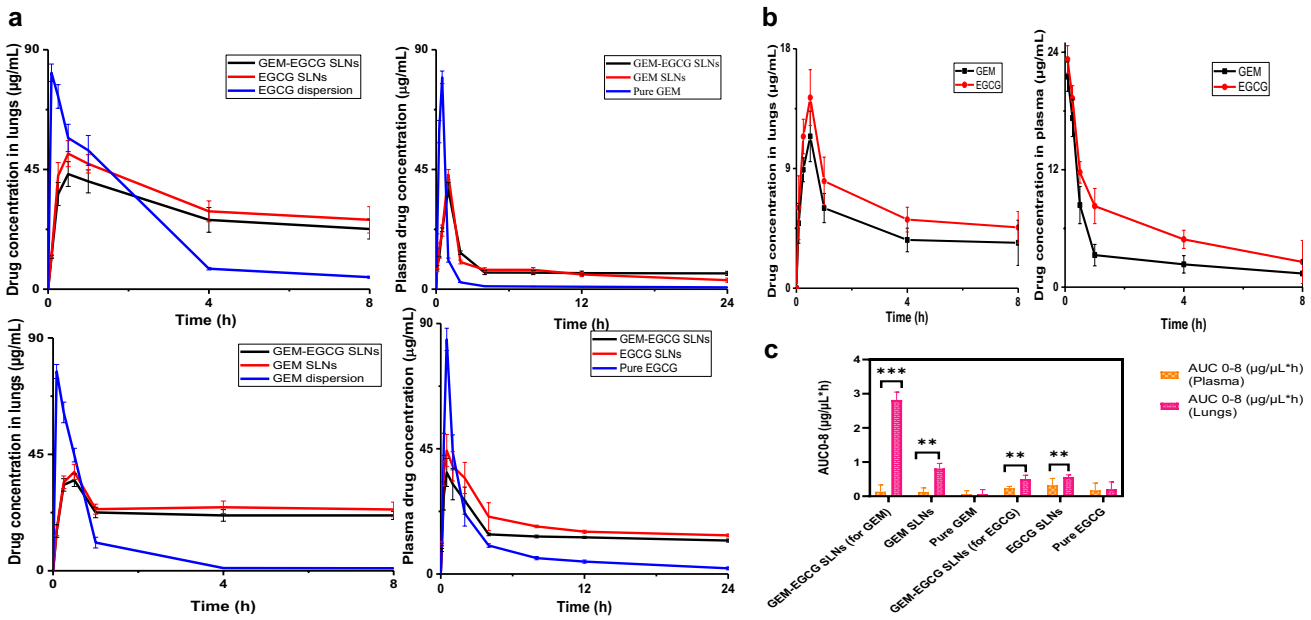

Fig. 3 **a** Pharmacokinetic profile of GEM and EGCG in plasma and lungs for GEM-EGCG SLNs, GEM SLNs, EGCG SLNs, pure GEM, and pure EGCG; **b** Pharmacokinetic profile of GEM and EGCG in lungs and plasma of mice after intravenous bolus administration of GEM-EGCG SLNs; and **c** Graphical representation of the comparison of $AUC_{0\text{-}8}$ for different formulations in plasma and lungs upon intranasal administration (Statistical values represent *** ($p < 0.001$), and ** ($p < 0.01$)) (abbreviations: GEM- gemcitabine; EGCG-epigallocatechin-3-gallate; GEM-EGCG SLNs- gemcitabine and epigallocatechin-3-gallate loaded solid lipid nanoparticles; GEM SLNs- gemcitabine loaded solid lipid nanoparticles; EGCG SLNs-epigallocatechin-3-gallate loaded solid lipid nanoparticles)

and degraded by plasma deaminase along with its elimination by liver and kidney which is not the case with intranasal administration, hence intranasal administration has resulted in greater concentration of GEM in the lungs. In comparison to GEM, the DTI value for EGCG is quite less which could account for the less biodistribution and elimination of EGCG after intravenous administration as compared to GEM [57, 58].

IVIS- *In vivo* Imaging System To evaluate the efficiency of the intranasal route for targeting the lungs, IVIS was used. The IVIS images in Fig. 4(b) show that the GEM-EGCG SLNs predominantly accumulated in the lungs at 0 h. At 1 h, they were present in the liver region, and from the 2nd hour, they were found in the kidney, intestines, and spleen due to rapid uptake by RES. The IVIS images at 24 and 48 h showed the presence of GEM-EGCG SLNs in the lungs, indicating a sustained drug release profile provided by GEM-EGCG SLNs. The results confirm that the intranasal route can be used to target the lungs effectively.

Biodistribution Study

Biodistribution studies were performed in female Wistar rats, 250 g ± 10 g, after 1 h and 6 h of intranasal administration to evaluate the targeting efficiency. The biodistribution results show that both drugs were randomly distributed to the liver within 1 h of intranasal administration. Pure GEM and pure EGCG showed higher biodistribution in the liver as compared to GEM-EGCG SLNs, GEM SLNs, and EGCG SLNs, which could be attributed to the sustained release of GEM and EGCG from SLNs and hinders rapid biodistribution whereas, in case of pure GEM and pure EGCG, the drug is free to be biodistributed rapidly in the body.

In comparison to the lungs, kidney, heart, and spleen, both drugs were found to be highly biodistributed in the liver, which could be reasoned as the liver is the main metabolizing organ for GEM and EGCG. Pure GEM was found to be present in high concentrations post 1 and 6 h in the liver, whereas GEM-EGCG SLNs and GEM SLNs have shown a fall-off in the biodistribution of GEM in the liver. A similar

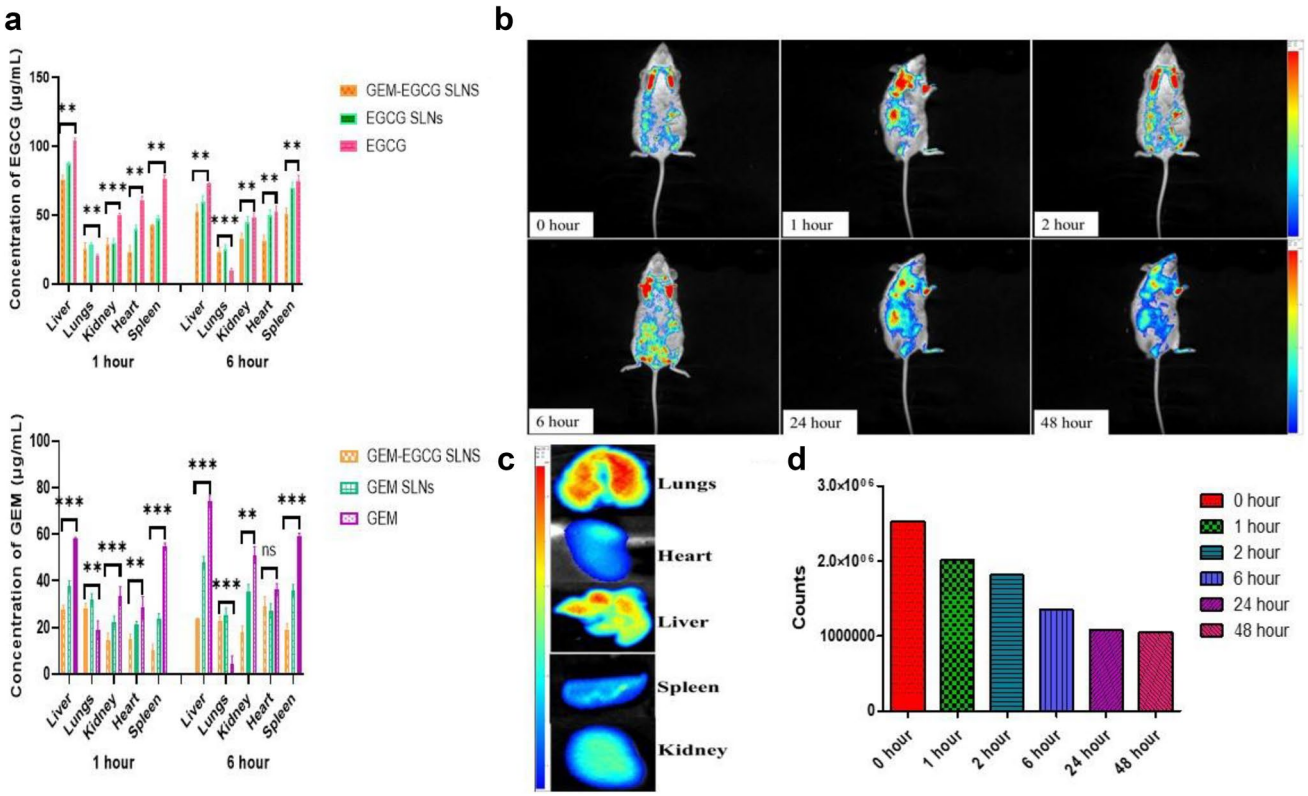

Fig. 4 **a** Bar diagram representation of relative biodistribution of GEM and EGCG in the vital organs after 1 h and 6 h of intranasal instillation of GEM-EGCG SLNs, EGCG SLNs, GEM SLNs, GEM, and EGCG; **b** IVIS images of mice after intranasal instillation of GEM-EGCG SLNs at different time points, depicting qualitative biodistribution of GEM-EGCG SLNs in the body; **c** IVIS images depicting biodistribution of GEM-EGCG SLNs in the vital organs after 48 h; **d** Graph representing ROI (region of interest) quantification in terms of bioluminescence signals of GEM-EGCG SLNs by IVIS imaging system in the lungs of mice at different time points. (statistical values represents *** ($p < 0.001$), ** ($p < 0.01$), and ns (non-significant)) (abbreviations: GEM- gemcitabine; EGCG- epigallocatechin-3-gallate; GEM-EGCG SLNs- gemcitabine and epigallocatechin-3-gallate loaded solid lipid nanoparticles; GEM SLNs- gemcitabine loaded solid lipid nanoparticles; EGCG SLNs- epigallocatechin-3-gallate loaded solid lipid nanoparticles)

pattern was observed for the biodistribution of EGCG from GEM-EGCG SLNs and EGCG SLNs in comparison to pure EGCG. The highest concentration was found to be present in the liver, kidney, and spleen which could be accredited to the fact that these are the major organs responsible for the metabolism of GEM [75] and EGCG [76] but it is comprehensible from Fig. 4(a) that the concentration of GEM and EGCG present in these major organs responsible for metabolism is less in case of GEM-EGCG SLNs, GEM SLNs, and EGCG SLNs as compared to pure GEM and pure EGCG, which signifies the protective effect of SLNs against biodistribution and hence clearance of drugs from the body [77]. The other possible justification for greater biodistribution of SLNs to the liver and spleen is rapid uptake by the reticuloendothelial system by the mechanism of endocytosis and phagocytosis. Lipidic systems are actively taken up by organs of the reticuloendothelial system [78–80]. The slow and sustained release of GEM and EGCG from SLNs hinders the process of biodistribution for GEM and EGCG and more amount of the drug is present at the desired site which is the lungs in the present study. SLNs are present in greater concentration in lungs as compared to pure GEM and pure EGCG because of the EPR effect of tumor cells which allows greater penetration of nanosized SLNs into lung tumor cells owing to their leaky vasculature and reduced drainage by the lymphatic system [81, 82].

Histopathological Study

Histological sections of mice represent adenocarcinoma-type lesions characterized by nests of cells corresponding to perforations kind of sieves as presented in Fig. 5(1). Moderate atypical adenomatous hyperplasia [83] in the bronchioles was observed in the histological sections from this group along with the thickening of the epithelium corresponding to epithelial hyperplasia (atypical adenomatous hyperplasia is the proliferation of columnar epithelial cells or cuboidal epithelial cells of bronchioles and alveoli of the respiratory tract. The lesions of atypical adenomatous hyperplasia correspond to a size of < 5 mm in diameter and are often multiple [84]). Images from treatment group GEM-EGCG SLNs show very few pathological lesions which support the

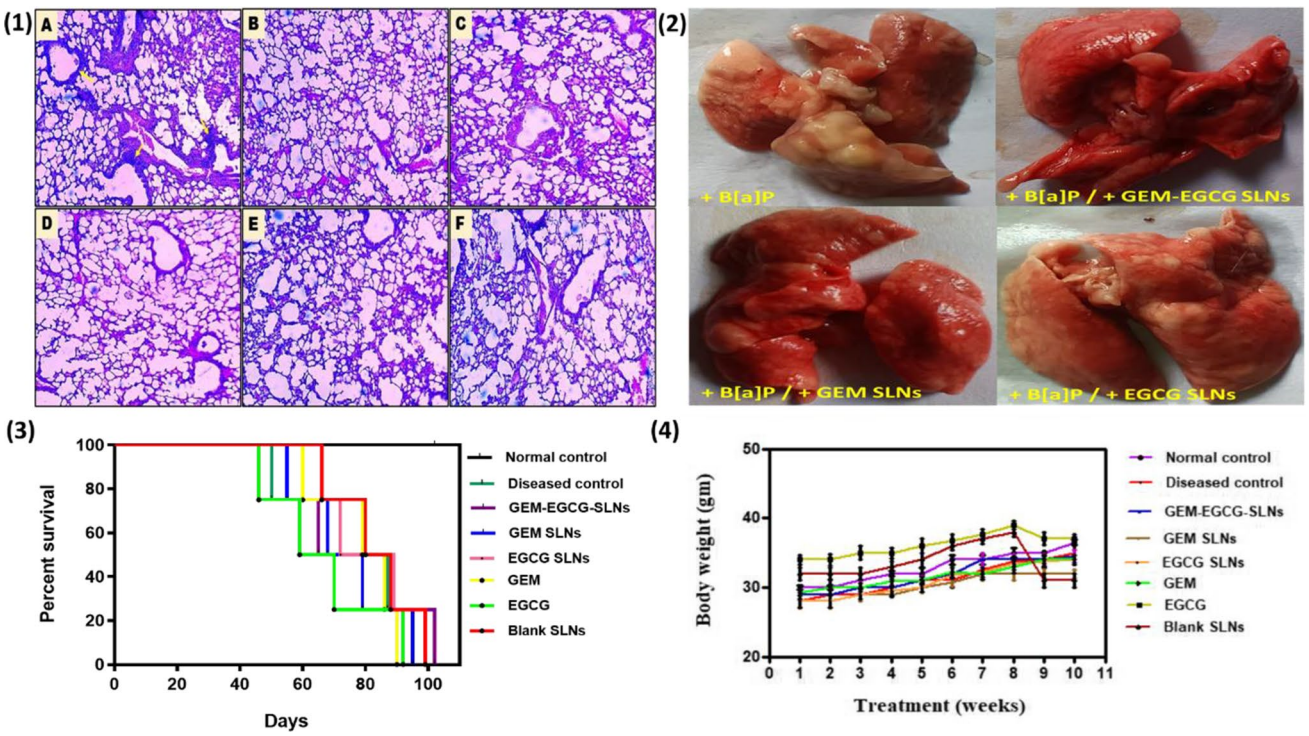

Fig. 5 1) Histological images from the groups- (**A**) diseased control group; (**B**) GEM-EGCG SLNs treatment group; (**C**) GEM SLNs treatment group; (**D**) EGCG SLNs treatment group(E) GEM drug control group; and (F) EGCG drug control group; (2) Images of lungs excised from different treatment groups at the end of study (3 months); (3) Survival analysis curve- Kaplan Meier curve, depicting the survival of different treatment groups over 100 days; (4) Curve depicting body weight changes in subjects from different treatment groups over the treatment period (abbreviations: GEM-gemcitabine; EGCG- epigallocatechin-3-gallate; GEM-EGCG SLNs- gemcitabine and epigallocatechin-3-gallate loaded solid lipid nanoparticles; GEM SLNs- gemcitabine loaded solid lipid nanoparticles; EGCG SLNs- epigallocatechin-3-gallate loaded solid lipid nanoparticles; blank SLNs- blank solid lipid nanoparticles; B[a]P- benzopyrene; + B[a]P- receiving benzopyrene; + B[a]P/ + GEM-EGCG SLNs- receiving benzopyrene and GEM-EGCG SLNs; + B[a]P/ + GEM SLNs- receiving benzopyrene and GEM-SLNs; + B[a]P/ + EGCG SLNs- receiving benzopyrene and EGCG SLNs)

potential of anti-tumor efficacy of GEM-EGCG SLNs as presented in Fig. 5(1-B).

Histological sections taken from the GEM drug control group and EGCG drug control group (Fig. 5(1-E & F)), represent mild atypical adenomatous hyperplasia in the bronchioles and epithelial hyperplasia [85, 86]. Histological sections from GEM SLNs treated group and EGCG SLNs treated group (Fig. 5(1-C & D)) represent regions of lesions with very slight atypical adenomatous hyperplasia contributing to the efficacy of monostearate-based SLNs as drug carrier and therapeutic potentials of GEM SLNs and EGCG SLNs when compared to GEM drug control and EGCG drug control group.

Assessment of Safety and Biocompatibility of SLNs

Histopathological investigation of the major organs viz., liver, and kidney (Fig. 6(a)) was performed to study any susceptibility of pathological lesions post intranasal administration of the saline (control group), and blank SLNs. The histological images from the control group and blank SLNs treated group confirm the safety of the monostearate-based SLNs carrier system as no pathological lesions were observed in the kidney and liver of the Swiss albino mice. Histological images of the kidney show clear glomerular cells and Bowman's capsule without any pathological lesions. The histological investigation postulates the safety of the formulation to be used in the study.

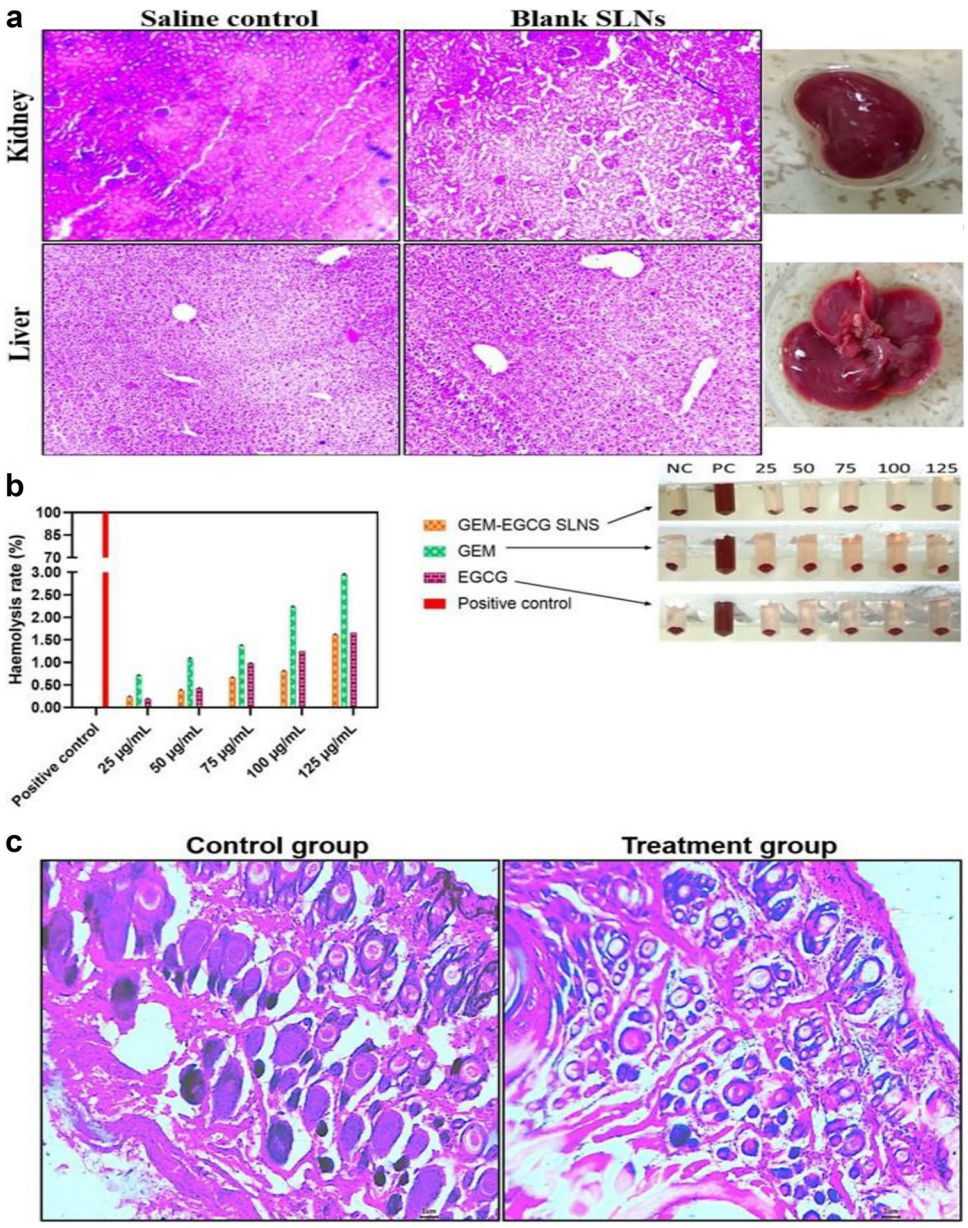

Fig. 6 **a** Histopathological images of the major metabolizing organs viz., kidney and liver to assess the safety of SLNs; **b** Bar graph representation of the hemolysis rate (%) at different concentrations of GEM-EGCG SLNs, GEM, EGCG, and positive control (triton X-100). The supporting photograph is from the experiment of the hemolysis study performed in different groups (NC: negative control; PC: positive control); and **c** Histopathological images of the nose of mice after intranasal instillation of GEM-EGCG SLNs (treatment group) compared with control group (abbreviations: GEM- gemcitabine; EGCG- epigallocatechin-3-gallate; GEM-EGCG SLNs- gemcitabine and epigallocatechin-3-gallate loaded solid lipid nanoparticles; blank SLNs- blank solid lipid nanoparticles)

Biocompatibility of GEM-EGCG SLNs with blood was assessed by a hemolysis study. Chemotherapy is often associated with hemolysis due to an interaction between drug particles with the membrane of erythrocyte which results in the lysis of erythrocyte cells along with enzyme degradation and hydrolysis [61]. We observed a hemolysis rate of $1.62 \pm 0.10\%$ for GEM-EGCG SLNs, $2.95 \pm 0.21\%$ for GEM, and $1.66 \pm 0.13\%$ for EGCG at a concentration of 125 µg/mL. Other dilutions of Gem-EGCG SLNs, GEM, and EGCG demonstrated very low values of hemolysis as represented in Fig. 6(b). The reduction in the rate of hemolysis for GEM-EGCG SLNs as compared to pure drug GEM and EGCG could be attributed to the presence of lipids and phospholipids in SLNs which provides a layer that acts as a shield on the surface and leads to attenuation of the hemolysis rate. Further, the drugs are present in the inner matrix of SLNs which prevent the interaction of GEM and EGCG with the membrane of erythrocyte cells [13].

Based on the hemolysis, histopathology, and biocompatibility studies wherein no pathological lesions and toxicity were observed in the eliminating organs, in the lungs, and blood, it can be suggested that the SLNs will be biocompatible with the nasal tissue. Moreover, the ingredients used (glyceryl monostearate, 1% polyvinyl alcohol, 1% pluronic F-127, and hydrogenated soy phosphatidylcholine) in the SLNs are 'GRAS certified' and are biocompatible and biodegradable. Further, the encapsulation of the drug in the SLNs does not directly expose the nasal tissue to the drug which might be toxic. Additionally, the design of the formulation allows only a small amount of drug release (if any) to occur at the nasal tissue because of the sustained release nature of the formulation. Moreover, following the intranasal administration of the formulation, we conducted a histological analysis of the nasal mucosa tissue (Fig. 6(c)). The study findings revealed that the nasal mucosa of the treatment group appeared normal compared to the control group that received no treatment. The columnar goblet cells and basal cells of the nasal epithelium were visible and had no distortion in morphology or shape. Moreover, the lamina propria region of the treatment group appeared normal with no distortion or pathological lesions in its structure, as compared to the histology image of the normal group [87, 88]. These results indicate that GEM-EGCG SLNs are safe for use in the nasal region of mice.

Conclusion

The results of the presented research demonstrate the potential of GEM-EGCG SLNs as a treatment approach against lung cancer. Epigallocatechin-3-gallate has synergistically aggravated the anti-cancer efficacy of gemcitabine against lung cancer. The DTI value signifies the caliber of the intranasal route of administration to target lungs which outweighs the dose-dependent side effects of chemotherapeutic drugs like GEM and also decreases the dose of these drugs as compared to the intravenous route of administration. The prepared monostearate-based lipidic nanoparticles are safe to use and biocompatible with no pathological lesion encountered in the kidney, liver, and nasal region of the Swiss Albino mice. The findings of our study pave the way for the exploration of the intranasal route of administration as a means of delivery of anticancer agents against lung cancer.

Author Contributions All authors contributed to the study conception and design. Material preparation, data collection and analysis were performed by Mohini Mishra. Figure and table mapping was performed by Aditya Sharma and Rinki Verma. Manuscript revision was done by Rinki Verma and Krishan Kumar. The first draft of the manuscript was written by Mohini Mishra and all authors commented on previous versions of the manuscript. Administration and supervision was done by Ruchi Chawla. All authors read and approved the final manuscript.

Funding No funding was received for this work.

Data Availability All data supporting the findings of this study are available within the paper.

Declarations

Conflict of Interest The authors report no financial and competing interest in the manuscript.

References

1. Kumar K, Rani V, Mishra M, Chawla R. New paradigm in combination therapy of siRNA with chemotherapeutic drugs for effective cancer therapy. Curr Res Pharmacol Drug Discov. 2022; 3. https://doi.org/10.1016/J.CRPHAR.2022.100103.
2. Siegel Mph RL, Giaquinto AN, Ahmedin I, Dvm J, Siegel RL. Cancer statistics, 2024. CA Cancer J Clin. 2024;74(1):12–49. https://doi.org/10.3322/CAAC.21820.
3. Siegel RL, Miller KD, Fuchs HE, Jemal A. Cancer statistics, 2022. CA Cancer J Clin. 2022;72(1):7–33. https://doi.org/10.3322/caac.21708.
4. Islami F, et al. Proportion and number of cancer cases and deaths attributable to potentially modifiable risk factors in the United States. CA Cancer J Clin. 2018;68(1):31–54. https://doi.org/10.3322/CAAC.21440.
5. Colby TV, Wistuba II, Gazdar A. Precursors to pulmonary neoplasia. Adv Anat Pathol. 1998;5(4):205–15. https://doi.org/10.1097/00125480-199807000-00001.
6. Gridelli C, et al. Non-small-cell lung cancer. Nat Rev Dis Prim. 2015;1:1–16. https://doi.org/10.1038/nrdp.2015.9.
7. Govindan R, et al. Changing epidemiology of small-cell lung cancer in the United States over the last 30 years: analysis of the surveillance, epidemiologic, and end results database. J Clin Oncol. 2006;24(28):4539–44. https://doi.org/10.1200/JCO.2005.04.4859.
8. Subramanian J, Govindan R. Lung cancer in never smokers: a review. J Clin Oncol. 2007;25(5):561–70. https://doi.org/10.1200/JCO.2006.06.8015.

9. Noble S, Goa KL. Gemcitabine. A review of its pharmacology and clinical potential in non-small cell lung cancer and pancreatic cancer. Drugs. 1997;54(3):447–72. https://doi.org/10.2165/00003495-199754030-00009.
10. Toschi L, Finocchiaro G, Bartolini S, Gioia V, Cappuzzo F. Role of gemcitabine in cancer therapy. Future Oncol. 2005;1(1):7–17. https://doi.org/10.1517/14796694.1.1.7.
11. Functional nucleoside transporters are required for gemcitabine influx and manifestation of toxicity in cancer cell lines - PubMed. [Online]. Available: https://pubmed.ncbi.nlm.nih.gov/9766663/. [Accessed: 17-Mar-2023].
12. Ciccolini J, Serdjebi C, Peters GJ, Giovannetti E. Pharmacokinetics and pharmacogenetics of Gemcitabine as a mainstay in adult and pediatric oncology: an EORTC-PAMM perspective. Cancer Chemother Pharmacol. 2016;78(1):1–12. https://doi.org/10.1007/s00280-016-3003-0.
13. Jeswani G, Alexander A, Saraf S, Saraf S, Qureshi A. Recent approaches for reducing hemolytic activity of chemotherapeutic agents. J Control Release. 2015;211:10–21. https://doi.org/10.1016/j.jconrel.2015.06.001.
14. Yang Y, Li N, Wang TM, Di L. Natural products with activity against lung cancer: A review focusing on the tumor microenvironment. Int J Mol Sci. 2021;22(19). https://doi.org/10.3390/ijms221910827.
15. Yang QQ, et al. Nanochemoprevention with therapeutic benefits: An updated review focused on epigallocatechin gallate delivery. Crit Rev Food Sci Nutr. 2020;60(8):1243–64. https://doi.org/10.1080/10408398.2019.1565490.
16. Demain AL, Vaishnav P. Natural products for cancer chemotherapy. Microb Biotechnol. 2011;4(6):687. https://doi.org/10.1111/J.1751-7915.2010.00221.X.
17. Hu J, Webster D, Cao J, Shao A. The safety of green tea and green tea extract consumption in adults – Results of a systematic review. Regul Toxicol Pharmacol. 2018;95:(August 2017):412–433. https://doi.org/10.1016/j.yrtph.2018.03.019.
18. Chakrawarti L, Agrawal R, Dang S, Gupta S. Expert opinion on therapeutic patents therapeutic effects of EGCG: a patent review. 2016;3776:(June). https://doi.org/10.1080/13543776.2016.1203419.
19. Meng X, et al. Identification and characterization of methylated and ring-fission metabolites of tea catechins formed in humans, mice, and rats. Chem Res Toxicol. 2002;15(8):1042–50. https://doi.org/10.1021/tx010184a.
20. Tang P, Sun Q, Yang H, Tang B, Pu H, Li H. Honokiol nanoparticles based on epigallocatechin gallate functionalized chitin to enhance therapeutic effects against liver cancer. Int J Pharm. 2018;545(1–2):74–83. https://doi.org/10.1016/j.ijpharm.2018.04.060.
21. Mishra M, Kumar P, Rajawat JS, Malik R, Sharma G, Modgil A. Nanotechnology: revolutionizing the science of drug delivery. Curr Pharm Des. 2019;24(43):5086–107. https://doi.org/10.2174/1381612825666190206222415.
22. Radhakrishnan R, et al. Encapsulation of biophenolic phytochemical EGCG within lipid nanoparticles enhances its stability and cytotoxicity against cancer. Chem Phys Lipids. 2016;198:51–60. https://doi.org/10.1016/J.CHEMPHYSLIP.2016.05.006.
23. Chawla R, Rani V, Mishra M. Nanoparticulate carriers—Versatile delivery systems. Nanopharm Adv Deliv Syst. 2021:31–54. https://doi.org/10.1002/9781119711698.CH2.
24. Zhang L, et al. Enhanced chemotherapeutic efficacy of plga-encapsulated epigallocatechin gallate (EGCG) against human lung cancer. Int J Nanomed. 2020;15:4417–29. https://doi.org/10.2147/IJN.S243657.
25. Bdair FM, Graham SP, Smith PF, Javle MM. Gemcitabine and acute myocardial infarction: a case report. Angiology. 2006;57(3):367–71. https://doi.org/10.1177/000331970605700314.
26. Hong Y, et al. Lung cancer therapy using doxorubicin and curcumin combination: Targeted prodrug based, pH sensitive nanomedicine. Biomed Pharmacother. 2019;112:108614. https://doi.org/10.1016/J.BIOPHA.2019.108614.
27. Chawla R, Sahu B, Mishra M, Rani V, Singh R. Intranasal micellar curcumin for the treatment of chronic asthma. J Drug Deliv Sci Technol. 2022;67:102922. https://doi.org/10.1016/J.JDDST.2021.102922.
28. Chen YJ et al. The synergistic anticancer effect of dual drug- (Cisplatin/Epigallocatechin Gallate) loaded gelatin nanoparticles for lung cancer treatment. J Nanomater 2020;2020. https://doi.org/10.1155/2020/9181549.
29. Wu J. The Enhanced Permeability and Retention (EPR) Effect: the significance of the concept and methods to enhance its application. J Pers Med. 2021;11(8). https://doi.org/10.3390/JPM11080771.
30. Wang J et al. Alantolactone enhances gemcitabine sensitivity of lung cancer cells through the reactive oxygen species-mediated endoplasmic reticulum stress and Akt / GSK3 β pathway. Int J Mol Med. 2019:1026–1038. https://doi.org/10.3892/ijmm.2019.4268.
31. Kumar K, et al. Dual targeting pH responsive chitosan nanoparticles for enhanced active cellular internalization of gemcitabine in non-small cell lung cancer. Int J Biol Macromol. 2023:126057. https://doi.org/10.1016/J.IJBIOMAC.2023.126057.
32. Plunkett W, Huang P, Xu YZ, Heinemann V, Grunewald R, Gandhi V. Gemcitabine: Metabolism, mechanisms of action, and self-potentiation. Semin Oncol. 1995;22(4 SUPPL. 11):3–10.
33. Granja A, Pinheiro M, Reis S. Epigallocatechin gallate nanodelivery systems for cancer therapy. Nutrients. 2016;8(5). https://doi.org/10.3390/nu8050307
34. Almatrood SA, Almatroudi A, Khan AA, Alhumaydh FA, Alsahl MA, Rahmani AH. Potential therapeutic targets of epigallocatechin gallate (EGCG), the most abundant catechin in green tea, and its role in the therapy of various types of cancer. Molecules. 2020;25(14). https://doi.org/10.3390/molecules25143146.
35. Shi J, Liu F, Zhang W, Liu X, Lin B, Tang X. Epigallocatechin-3-gallate inhibits nicotine-induced migration and invasion by the suppression of angiogenesis and epithelial-mesenchymal transition in non-small cell lung cancer cells. Oncol Rep. 2015;33(6):2972–80. https://doi.org/10.3892/or.2015.3889.
36. Lemarie E, et al. Aerosolized gemcitabine in patients with carcinoma of the lung: Feasibility and safety study. J Aerosol Med Pulm Drug Deliv. 2011;24(6):261–70. https://doi.org/10.1089/jamp.2010.0872.
37. Mi FL, et al. Active tumor-targeted co-delivery of epigallocatechin gallate and doxorubicin in nanoparticles for combination gastric cancer therapy. ACS Biomater Sci Eng. 2018;4(8):2847–59. https://doi.org/10.1021/ACSBIOMATERIALS.8B00242.
38. Duan Y, et al. A brief review on solid lipid nanoparticles: part and parcel of contemporary drug delivery systems. RSC Adv. 2020;10(45):26777–91. https://doi.org/10.1039/D0RA03491F.
39. Chaurawal N, et al. Oral sorafenib-loaded microemulsion for breast cancer: evidences from the in-vitro evaluations and pharmacokinetic studies. Sci Rep. 2022;12(1):13746. https://doi.org/10.1038/S41598-022-17333-6.
40. Hao Y, Zhao F, Li N, Yang Y, Li K. Studies on a high encapsulation of colchicine by a niosome system. Int J Pharm. 2002;244(1–2):73–80. https://doi.org/10.1016/S0378-5173(02)00301-0.
41. Guimarães Sá Correia M, Briuglia ML, Niosi F, Lamprou DA. Microfluidic manufacturing of phospholipid nanoparticles: stability, encapsulation efficacy, and drug release. Int J Pharm. 2017;516(1–2):91–99. https://doi.org/10.1016/J.IJPHARM.2016.11.025.

42. Jain A, et al. Beta-carotene-Encapsulated Solid Lipid Nanoparticles (BC-SLNs) as promising vehicle for cancer: an investigative assessment. AAPS PharmSciTech. 2019;20(3):1–7. https://doi.org/10.1208/S12249-019-1301-7/TABLES/3.
43. Amreddy N, et al. Tumor-targeted and pH-controlled delivery of doxorubicin using gold nanorods for lung cancer therapy. Int J Nanomed. 2015;10:6773–88. https://doi.org/10.2147/IJN.S93237.
44. Almurshedi AS, et al. A novel pH-sensitive liposome to trigger delivery of afatinib to cancer cells: Impact on lung cancer therapy. J Mol Liq. 2018;259:154–66. https://doi.org/10.1016/J.MOLLIQ.2018.03.024.
45. Pang J, Xing H, Sun Y, Feng S, Wang S. Non-small cell lung cancer combination therapy: hyaluronic acid modified, epidermal growth factor receptor targeted, pH sensitive lipid-polymer hybrid nanoparticles for the delivery of erlotinib plus bevacizumab. Biomed Pharmacother. 2020;125:109861. https://doi.org/10.1016/j.biopha.2020.109861.
46. Verma R, Singh V, Koch B, Kumar M. Evaluation of methotrexate encapsulated polymeric nanocarrier for breast cancer treatment. Colloids Surf B Biointerfaces. 2023;226. https://doi.org/10.1016/J.COLSURFB.2023.113308.
47. Kasala ER, Bodduluru LN, Barua CC, Sriram CS, Gogoi R. Benzo(a)pyrene induced lung cancer: role of dietary phytochemicals in chemoprevention. Pharmacol Rep. 2015;67(5):996–1009. https://doi.org/10.1016/J.PHAREP.2015.03.004.
48. Swauger JE, Steichen TJ, Murphy PA, Kinsler S. An analysis of the mainstream smoke chemistry of samples of the U.S. cigarette market acquired between 1995 and 2000. Regul Toxicol Pharmacol. 2002;35(2):142–56. https://doi.org/10.1006/RTPH.2001.1521.
49. Sinha R, Kulldorff M, Gunter MJ, Strickland P, Rothman N. Dietary benzo[a]pyrene intake and risk of colorectal adenoma. Cancer Epidemiol Biomarkers Prev. 2005;14(8):2030–4. https://doi.org/10.1158/1055-9965.EPI-04-0854.
50. Alexandrov K, Rojas M, Satarug S. The critical DNA damage by benzo(a)pyrene in lung tissues of smokers and approaches to preventing its formation. Toxicol Lett. 2010;198(1):63–8. https://doi.org/10.1016/J.TOXLET.2010.04.009.
51. Hecht SS. Tobacco carcinogens, their biomarkers and tobacco-induced cancer. Nat Rev Cancer. 2003;3(10):733–44. https://doi.org/10.1038/NRC1190.
52. Vikis HG, Rymaszewski AL, Tichelaar JW. Mouse models of chemically-induced lung carcinogenesis. Front Biosci (Elite Ed). 2013;5(3):939–46. https://doi.org/10.2741/E673.
53. Sikdar S, et al. Post-cancer treatment with condurango 30C shows amelioration of benzo[a]pyrene-induced lung cancer in rats through the molecular pathway of Caspa- se-3-mediated apoptosis induction: -Anti-lung cancer potential of Condurango 30C in rats-. J Pharmacopuncture. 2013;16(3):11. https://doi.org/10.3831/KPI.2013.16.021.
54. Monteillier A, Voisin A, Furrer P, Allémann E, Cuendet M. Intranasal administration of resveratrol successfully prevents lung cancer in A/J mice. Sci Rep. 2018;8(1):1–9. https://doi.org/10.1038/s41598-018-32423-0.
55. Lemarie E, et al. Aerosolized gemcitabine in patients with carcinoma of the lung: feasibility and safety study. J Aerosol Med Pulm Drug Deliv. 2011;24(6):261–70. https://doi.org/10.1089/JAMP.2010.0872.
56. Estimating the maximum safe starting dose in initial clinical trials for therapeutics in adult healthy volunteers | FDA. [Online]. Available: https://www.fda.gov/regulatory-information/search-fda-guidance-documents/estimating-maximum-safe-starting-dose-initial-clinical-trials-therapeutics-adult-healthy-volunteers. [Accessed: 14-Jan-2023].
57. Furubayashi T, Inoue D, Kimura S, Tanaka A, Sakane T. Evaluation of the pharmacokinetics of intranasal drug delivery for targeting cervical lymph nodes in rats. Pharmaceutics. 2021;13(9):1–9. https://doi.org/10.3390/pharmaceutics13091363.
58. Stevens AJ, Martin SW, Brennan BS, Rowland M, Houston JB. Experimental determination of a drug targeting index for s(+ibuprofen using the rat air pouch model of inflammation. J Drug Target. 1994;2(4):333–9. https://doi.org/10.3109/10611869409015914.
59. Mohammed F, et al. ROS-responsive polymeric nanocarriers with photoinduced exposure of cell-penetrating moieties for specific intracellular drug delivery. ACS Appl Mater Interfaces. 2019;11(35):31681–92. https://doi.org/10.1021/ACSAMI.9B10950.
60. Verma R, Rani V, Kumar M. In-vivo anticancer efficacy of self-targeted methotrexate-loaded polymeric nanoparticles in solid tumor-bearing rat. Int Immunopharmacol. 2023;119. https://doi.org/10.1016/J.INTIMP.2023.110147.
61. Dobrovolskaia MA, Clogston JD, Neun BW, Hall JB, Patri AK, McNeil SE. Method for analysis of nanoparticle hemolytic properties in vitro. Nano Lett. 2008;8(8):2180–7. https://doi.org/10.1021/nl0805615.
62. Mazzarino L, Loch-Neckel G, Dos Santos Bubniak L, Ourique F, Otsuka I, Halila S, Curi Pedrosa R, Santos-Silva MC, Lemos-Senna E, Curti Muniz E, Borsali R. Nanoparticles made from xyloglucan-block-polycaprolactone copolymers: safety assessment for drug delivery. Toxicol Sci. 2015;147(1):104–15. https://doi.org/10.1093/toxsci/kfv114.
63. Le Guellec S, Ehrmann S, Vecellio L. *In vitro – in vivo* correlation of intranasal drug deposition. Adv Drug Deliv Rev. 2021;170:340–52. https://doi.org/10.1016/J.ADDR.2020.09.002.
64. Labiris NR, Dolovich MB. Pulmonary drug delivery. Part I: physiological factors affecting therapeutic effectiveness of aerosolized medications. Br J Clin Pharmacol. 2003;56(6):588. https://doi.org/10.1046/J.1365-2125.2003.01892.X.
65. Jabbal S, Poli G, Lipworth B. Does size really matter?: Relationship of particle size to lung deposition and exhaled fraction. J Allergy Clin Immunol. 2017;139(6):2013-2014.e1. https://doi.org/10.1016/j.jaci.2016.11.036.
66. Heyder J. Deposition of inhaled particles in the human respiratory tract and consequences for regional targeting in respiratory drug delivery. Proc Am Thorac Soc. 2004;1(4):315–20. https://doi.org/10.1513/PATS.200409-046TA.
67. Effros RM, Mason GR. Measurements of pulmonary epithelial permeability *in vivo*. Am Rev Respir Dis. 1983;127(5 Pt 2):S59-65.
68. Folkesson HG, Westrom BR, Karlsson BW. Permeability of the respiratory tract to different-sized macromolecules after intratracheal instillation in young and adult rats. Acta Physiol Scand. 1990;139(1–2):347–54. https://doi.org/10.1111/J.1748-1716.1990.TB08933.X.
69. Bahadur S, Pardhi DM, Rautio J, Rosenholm JM, Pathak K. Intranasal nanoemulsions for direct nose-to-brain delivery of actives for CNS disorders. Pharmaceutics. 2020;12(12):1–27. https://doi.org/10.3390/PHARMACEUTICS12121230.
70. Formica ML, Real DA, Picchio ML, Catlin E, Donnelly RF, Paredes AJ. On a highway to the brain: a review on nose-to-brain drug delivery using nanoparticles. Appl Mater Today. 2022;29:101631. https://doi.org/10.1016/J.APMT.2022.101631.
71. Aderibigbe BA, Naki T. Design and efficacy of nanogels formulations for intranasal administration. Mol. 2018;23(6):1241. https://doi.org/10.3390/MOLECULES23061241.
72. Far J, Abdel-Haq M, Gruber M, Abu Ammar A. Developing biodegradable nanoparticles loaded with mometasone furoate for potential nasal drug delivery. ACS Omega. 2020;5(13):7432–7439. https://doi.org/10.1021/ACSOMEGA.0C00111/ASSET/IMAGES/LARGE/AO0C00111_0002.JPEG.

73. Verma R, Kumar M. Development and optimization of methotrexate encapsulated polymeric nanocarrier by ionic gelation method and its evaluations. ChemistrySelect 2022;7(48). https://doi.org/10.1002/SLCT.202203698.
74. Deshmukh M, et al. Biodistribution and renal clearance of biocompatible lung targeted Poly(ethylene glycol) (PEG) nanogel aggregates. J Control Release. 2012;164(1):65–73. https://doi.org/10.1016/J.JCONREL.2012.09.011.
75. Plunkett W, Huang P, Xu YZ, Heinemann V, Grunewald R, Gandhi V. Gemcitabine: metabolism, mechanisms of action, and self-potentiation. Semin Oncol. 1995;22(4 Suppl 11):3–10.
76. Legeay S, Rodier M, Fillon L, Faure S, Clere N. Epigallocatechin gallate: a review of its beneficial properties to prevent metabolic syndrome. Nutrients. 2015;7(7):5443. https://doi.org/10.3390/NU7075230.
77. Celia C, Cosco D, Paolino D, Fresta M. Gemcitabine-loaded innovative nanocarriers vs GEMZAR: biodistribution, pharmacokinetic features and *in vivo* antitumor activity. 2011;8(12):1609–1629. https://doi.org/10.1517/17425247.2011.632630.
78. Manjunath K, Venkateswarlu V. Pharmacokinetics, tissue distribution and bioavailability of clozapine solid lipid nanoparticles after intravenous and intraduodenal administration. J Control Release. 2005;107(2):215–28. https://doi.org/10.1016/J.JCONREL.2005.06.006.
79. Mizushima Y, Hamano T, Yokoyama K. Tissue distribution and anti-inflammatory activity of corticosteroids incorporated in lipid emulsion. Ann Rheum Dis. 1982;41(3):263–7. https://doi.org/10.1136/ARD.41.3.263.
80. Li S, Ji Z, Zou M, Nie X, Shi Y, Cheng G. Preparation, characterization, pharmacokinetics and tissue distribution of solid lipid nanoparticles loaded with tetrandrine. AAPS PharmSciTech. 2011;12(3):1011–8. https://doi.org/10.1208/S12249-011-9665-3/FIGURES/6.
81. Greish K. Enhanced Permeability and Retention (EPR) effect for anticancer nanomedicine drug targeting. Methods Mol Biol. 2010;624:25–37. https://doi.org/10.1007/978-1-60761-609-2_3.
82. Nakamura Y, Mochida A, Choyke PL, Kobayashi H. Nanodrug delivery: is the enhanced permeability and retention effect sufficient for curing cancer? Bioconjug Chem. 2016;27(10):2225–38. https://doi.org/10.1021/ACS.BIOCONJCHEM.6B00437/ASSET/IMAGES/MEDIUM/BC-2016-00437T_0005.GIF.
83. Wang Y, et al. Analysis of lung tumor initiation and progression in transgenic mice for Cre-inducible overexpression of Cul4A gene. Thorac cancer. 2015;6(4):480–7. https://doi.org/10.1111/1759-7714.12257.
84. Travis WD. Pathology of lung cancer. Clin Chest Med. 2002;23(1):65–81. https://doi.org/10.1016/S0272-5231(03)00061-3.
85. Solis LM, et al. Histologic patterns and molecular characteristics of lung adenocarcinoma associated with clinical outcome. Cancer. 2012;118(11):2889. https://doi.org/10.1002/CNCR.26584.
86. Inamura K. Lung cancer: understanding its molecular pathology and the 2015 WHO Classification. Front Oncol. 2017;7(AUG):193. https://doi.org/10.3389/FONC.2017.00193.
87. Bojsen-Møller F. Topography of the nasal glands in rats and some other mammals. Anat Rec. 1964;150(1):11–24. https://doi.org/10.1002/AR.1091500103.
88. Chamanza R, Wright JA. A review of the comparative anatomy, histology, physiology and pathology of the nasal cavity of rats, mice, dogs and non-human primates. relevance to inhalation toxicology and human health risk assessment. J Comp Pathol. 2015;153(4):287–314. https://doi.org/10.1016/J.JCPA.2015.08.009.